

Tunable, bandwidth controllable source of THz radiation

A. Zigler, D. Hashimshony and K. Papadopoulos

Abstract: Tunable radiation in the range from 0.1 to a few THz by the interaction of a superluminous photoconducting front with an electrostatic 'frozen wave' configuration in a semiconductor is reported. The interaction converts the energy contained in the 'frozen wave' into THz radiation, whose frequency depends on the energy in the laser pulse creating the superluminous front and the wavelength of the static wave. Use of two-photon absorption leads to a volume interaction, creating a superluminous photoconducting front. Tunability was achieved by varying the laser pulse energy from 0.1 to 1 mJ. Power scaling as a function of the electrostatic 'frozen wave' energy was obtained. The capability of the concept to act as a narrow or wideband, tunable and powerful THz source is demonstrated.

1 Introduction

The THz/FIR region of the electromagnetic spectrum has a unique utility in characterising electronic, vibrational and compositional properties of solids, liquids, gases, flames and flows [1, 2]. Lack of powerful, coherent, narrowband and tunable radiation sources in this frequency range has prevented its extensive utilisation. The availability of femtosecond lasers has recently led to the development of new types of THz sources based on the principle of DC to AC conversion. Powerful, broadband THz radiation was generated by the incidence of 100 fs laser pulses on large aperture monotonically biased photoconductors, such as GaAs [1–10]. The broadband radiation pattern generated by this technique is controlled only by the laser pulse risetime and the relaxation properties of the carriers. Two physical mechanisms have been advanced as the source of the radiation: photoconduction [3–6] and optical rectification [3, 7–10]. Photoconduction relies on high-speed photoconductors generating transient current sources as radiating antennas. Optical rectification relies on a second order nonlinear optical process induced by the presence of a DC electric field. In both cases the physics underlying the process involves surface rather than volume interaction.

Generation of short bursts of monochromatic radiation in the lower frequency range between 5 and 20 GHz was recently reported [12, 13] by a variant approach that utilises a frozen wave configuration in a neutral gas (azulene vapour) that is subsequently ionised by a 266 nm laser pulse.

Here we present a proof-of-principle experiment of a radiation process whose underlying physics combines elements of the approaches described previously. Key new elements include:

- volume rather than surface interaction between the laser and the charged photoconducting configuration. This is accomplished by using a two-photon absorption process
- generation of the transient radiation inside the plasma rather than in free space. This is achieved by using oblique incidence of the laser front to achieve a superluminous ionising front.

These require that the emitted radiation frequency is consistent with the dispersion properties of the plasma generated in the photoconductor volume, and the wavelength and number of the frozen waves involved in the interaction. Primary control of the radiation frequency is adjusting the plasma frequency, which is a linear function of the energy in the laser pulse. Further frequency tuning can be achieved by changing the wavelength of the frozen wave or the angle of incidence of the laser front. The radiation bandwidth is a function of the number of frozen waves contained in the photoconductor.

The experiment, conducted using the computerised set-up shown in Fig. 1, presents the full control over the emitted radiation spectrum, bandwidth and time domain profile. All set-up parameters such as optical delay position, sampling rate and scan length were controlled, and all the collected information during the scan was recorded and displayed online by the computer.

The miniature photoconducting capacitor array (MPCA) unit built consists of ten frozen waves, which were connected to the switchboard so that the operator could predetermine the 'frozen' wave profile. We used a $20 \times 1 \times 0.5$ (mm)³ crystal to form the array shown in Fig. 2. Using the maximum number of 20 capacitors (10 frozen waves) we obtain a relatively narrow bandwidth for the initial field and as a consequence a narrow radiation spectrum. The gap between neighbouring capacitors was 0.5 mm. The distance between capacitor plates was 0.5 mm, filled with ZnSe photoconductive crystal. Each capacitor was connected to the DC external source (up to

© IEE, 2002

IEE Proceedings online no. 20020535

DOI: 10.1049/jip-opt:20020535

Paper first received 2nd November 2001 and in revised form 29th April 2002

A. Zigler and D. Hashimshony are with the Racah Institute of Physics, Hebrew University, Jerusalem, Israel
K. Papadopoulos is with the University of Maryland, College Park, MD 20740, USA

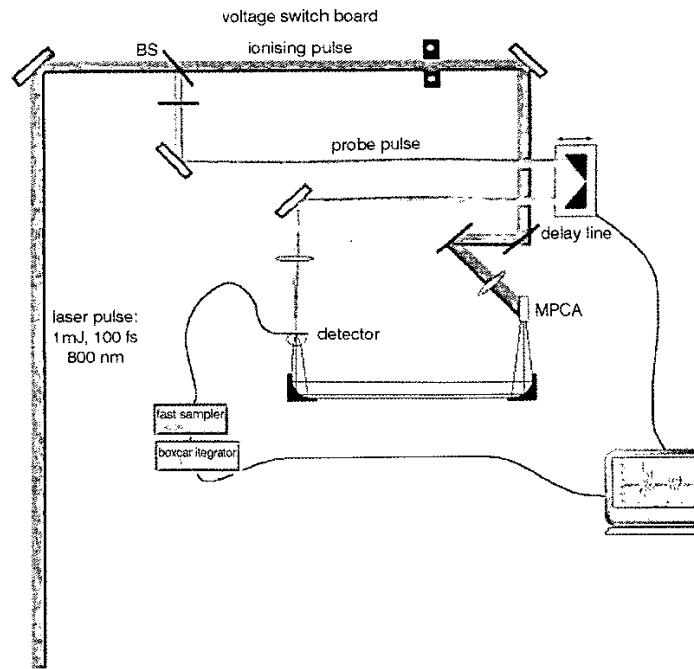


Fig. 1 Experimental set-up

100 V) independently of the connection of other capacitors. This allowed the construction of almost any required profile for the initial static electric field inside the crystal.

The experiments were conducted using a 100 fs Ti:sapphire laser operating at 0.8 μm and repetition rate 10 Hz. The waveform of the radiated electric field was measured using the standard pump and probe technique [14]. The laser beam was split into two beams. The main beam carrying more than 90% of the energy served as the pump beam and the second beam served as the probe beam. The main beam was focused by a cylindrical lens on the side of the ZnSe crystal to form the propagating ionising front. The crystal was placed at an angle of 20 degrees to the pump laser beam front. At this angle, the refracted beam inside the crystal is penetrating at an angle of about 9 degrees to the crystal surface. This illumination geometry generates an ionisation front propagating inside the crystal at a superluminal speed. The probing beam reflected from the beam splitter and was directed to a retro-reflector and then focused on the detector. The retro-reflector was placed on a stage connected to a step motor, which can move the stage with a submicron step size. An encoder records the exact position of the stage and the information was recorded by a computer. A gated planar dipole antenna monitored the amplitude of the radiated electric field. The initial optical paths of the two beams were adjusted so that both beams would reach the detector at the same time. The dipole antenna was constructed on a heavily ion-implanted silicon layer of a SOS wafer. The implantation resulted in a subpicosecond

temporal response due to reduction of the recombination time. The antenna detector was gated at different delay times by varying the optical delay between the pump and probe laser pulses. The antenna was driven by the radiation from the capacitor array. The amplitude of the induced, time-dependent voltage across the gap was determined by measuring the average current produced in the antenna circuit.

This current flows through the detector only when the gap is irradiated and shorted by the delayed 100 fs laser probe beam. An SRS250 boxcar integrator was used to collect the short current pulses. The current was averaged over many pulses until additional averaging did not change the moving average value by more than 3%. The maximum number of averaged pulses was 10 000, limited only by the integrator. This results in an averaging of 100–10 000 pulses for each delay stop. A full scan contained about 120 delay points. The number of points and the sampling resolution were predetermined by the expected emission frequency and the corresponding Nyquist frequency. As a result, a full scan lasted from 30 to 180 min. The profile of the radiation electric field was determined by monitoring the averaged current against the time delay between the pump laser beam and the probe laser beam. The repetition rate was limited by the laser system only. Working in a 10 Hz repetition rate made the measurement extremely sensitive to the environmental conditions and long-term laser stability.

The ZnSe crystal was cut and polished to the shape shown in Fig. 2. The crystal was chosen so that its energy gap (2.4 eV) is larger than the energy of the single photon of the

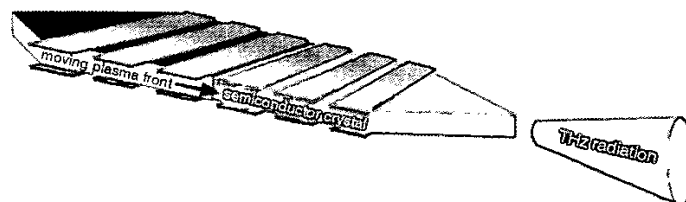


Fig. 2 Radiating structure

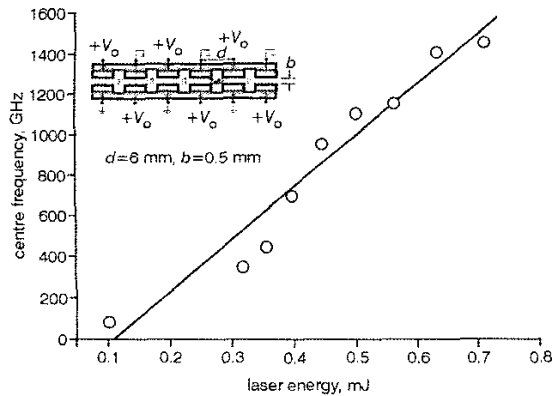


Fig. 3 Frequency tuning as function of illumination energy
Capacitors are charged to 40 V. It is clear that the frequency of the radiation scales linearly with the energy in the laser pulse

laser. As a result, the carrier generation involves two photons and the absorption depth is intensity-dependent. The absorption of the crystal used in the experiment was measured experimentally. For laser intensities above 10^{10} W/cm², all energy was absorbed; at low laser intensities the crystal was transparent. This allows for deeper penetration of the laser radiation and creation of a large volume of carriers, resulting in a volume interaction of the front with the bias rather than the surface interaction occurring in the large aperture antennas referred to previously. It should be noted that, in [12, 13], two-photon absorption was used due to the ionisation energy requirement of the gaseous medium. Contrary to this, in our case we could have chosen a single- or two-photon absorption (by a proper choice of the crystal). Single-photon absorption would have resulted in plasma thickness smaller than c/ω_e and the relevant wave would be a surface wave with relatively low eigenfrequency. By selecting two-photon absorption the plasma thickness is larger than c/ω_e and the wave driven by the interaction is a volume plasma wave whose eigenfrequency equals the plasma frequency as given by the dispersion relation of (1).

2 Results

Using this system we have studied the radiation frequency and power scaling as functions of laser energy and voltage on the capacitor structure. The obtained results are shown in Figs. 3 and 4. It is clear that the frequency of the radiation scales linearly with the energy in the laser pulse. Scaling properties of the proposed concept with respect to

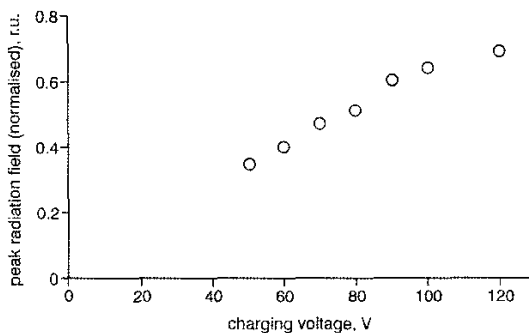


Fig. 4 Radiating field as function of voltage on capacitor structure

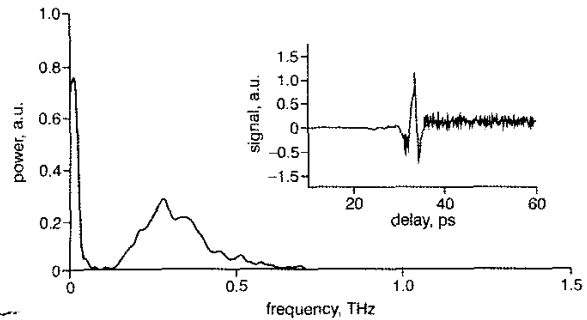


Fig. 5 Wideband radiation

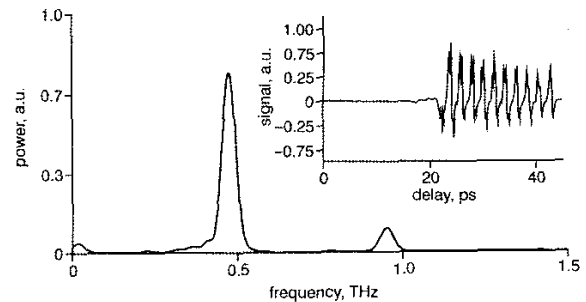


Fig. 6 Narrowband THz radiation

the radiation bandwidth and the possibility of waveform modulation were studied by charging various numbers of capacitors. Examples of narrow and broadband radiation are presented in Figs. 5 (four alternately charged capacitors) and 6 (20 alternately charged capacitors). The bandwidth narrowing is proportional to the number of connected capacitors. For the convenience of interpretation both the frequency and the time domains are presented. In the case of non-sequential connection the amplitude of the emitted radiation is modulated as shown in Fig. 7. Only the

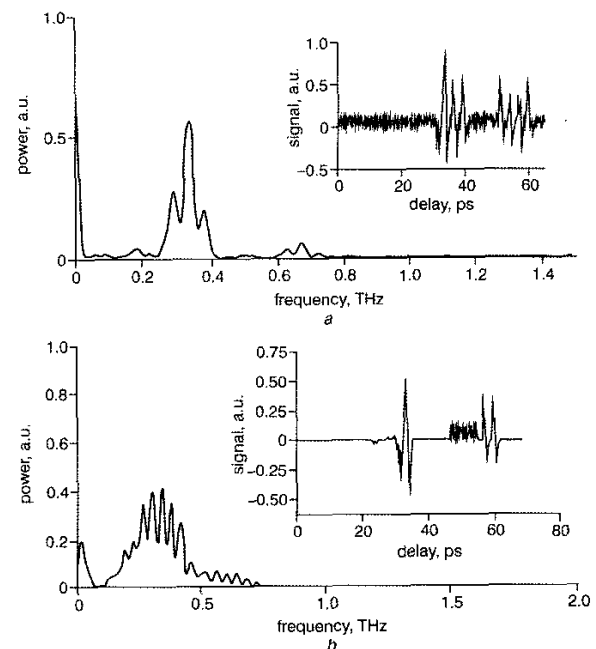


Fig. 7 Spectrum modulation

first four capacitors and last two capacitors were charged in the case illustrated in Fig. 7a and eight and six in Fig. 7b; the rest are connected to the ground.

3 Discussion

In interpreting and scaling the above results it is instructive to refer to the traditional frozen wave generator concept [1, 2, 4–6]. Such a device consists of segments of transmission line sections with one-way transit times equal to the desired microwave half-period arranged in series or parallel and connected with optically activated switches. The sections are charged alternatively positive and negative to form a DC ‘frozen-wave’. Radiation is produced when the optically controlled switches are activated simultaneously. The critical differences in the physics controlling our device and the traditional frozen wave generator are that the shorting of the capacitor array is sequential and the resultant radiation propagates inside the plasma which is generated at superluminal speeds. This, however, has profound consequences since the frequency is upshifted to satisfy the appropriate dispersion relation and phase matching conditions. Following Lampe and other workers [15–20] we work in the laboratory frame since the front is superluminal. There are three modes in the system. The first is the frozen wave, with zero frequency and wavelength $k_0 = \pi/d$, where d is the distance between the capacitors. The other two are the right (+) and left (–) propagating waves in the semiconductor plasma. They must satisfy the usual dispersion relation

$$k_{1,2}c/\omega = \varepsilon^{1/2} \{1 - (\omega_e^2/\omega_{1,2}^2)[\omega_{1,2}/(\omega_{1,2} - i\gamma)]\}^{1/2} \quad (1)$$

where ε is the dielectric constant of the semiconductor, ω_e is the plasma frequency and γ the phenomenological dephasing rate [3]. The continuity conditions require that the waves are in phase at the front, $z = -Ut$, where $U = c/\sin\theta$ and θ is the incidence angle of the laser on the semiconductor. This gives

$$k_0c/\sin\theta = \omega_{1,2} + k_{1,2}c/\sin\theta \quad (2)$$

Notice that the direction of $k_{1,2}$ is the direction of the ionisation front, i.e. the direction of the crystal axis and not the direction of the incident lightwave whose sole purpose is to ionise, and does not participate in the interaction. This is clearly explained in Lampe *et al.* [16].

Neglecting the leftward wave since it never catches up with the front [15–20] and dropping the subscript from the frequency and wavenumber of the forward wave, we find from (1) and (2) the relationship between the emitted frequency ω and the other parameters as

$$(k_0c\beta - \omega)^2 - \omega^2\varepsilon\beta^2 + \omega_e^2\varepsilon\beta^2 \frac{\omega}{\omega - i\gamma} = 0 \quad (3)$$

where $\beta = 1/\sin\theta$. It is easy to see that, in the absence of plasma, i.e. $\omega_e \geq 0$ (or $\omega \gg \omega_e$), (3) reduces to the frozen generator equation. However, for $k_0c\beta \ll \omega$, (3) becomes

$$\omega(\omega - i\gamma) = \omega_e^2 \frac{\varepsilon\beta^2}{\varepsilon\beta^2 - 1} \quad (4)$$

It is clear that for $\omega_e \gg \gamma$ and $\varepsilon\beta^2 \gg 1$, conditions easily fulfilled in our experiment, the emitted frequency ω is near the plasma frequency and proportional to n , where n is the carrier density, $\omega_e \sim \sqrt{n}$. The value of n is, of course, a function of the laser energy per pulse W . It is easy to see that, for two-photon absorption, since the absorption length is $(\alpha I)^{-1}$, where I is the laser intensity and α the

two-photon absorption coefficient, the average density is given by

$$n = \alpha W^2/h\nu S^2\tau \quad (5)$$

where S is the illuminated area of the crystal and τ the laser pulse length. From (4) and (5) we find that the emitted frequency scales linearly with the laser pulse energy, consistent with our experimental results presented in Fig. 3.

The scaling properties of the concept were analysed with respect to power, frequency and bandwidth. As noted in Lampe *et al.* [16] for superluminal fronts, the transmission coefficient is close to unity. As a result the output radiation has field amplitude close to the static field. During the sweep time the electrostatic energy stored in the photoconductor is transformed into electromagnetic radiation. The energy stored in a photoconductor of length l , area S , composed of N capacitors occupying a fraction f of the volume with a DC field E_0 is given by

$$K = (1/2)f\varepsilon\varepsilon_0E_0^2(Sl)$$

The discharge time $t = 1/V_g$, where V_g is the group velocity of the radiation. Approximating $(1/2)f\varepsilon$ by unity, we find that the maximum power density P will be given by

$$P = 10^5(V_g/c)(E_0/10 \text{ kV/cm})^2 \text{ W/cm}^2 \quad (6)$$

The E^2 power scaling shows clearly the potential for producing high power radiation. Using a relatively conservative value of 10 kV/cm (that is lower than the breakdown threshold) in $K = (1/2)f\varepsilon\varepsilon_0E_0^2(Sl)$, with $(1/2)f\varepsilon$ of order unity, one can estimate the stored energy of about $10 \mu\text{J/cm}^3$. To generate 1 THz radiation we need 5×10^{15} electrons per cm^3 that will require 2.7 eV per electron and a total of $\sim 1 \text{ mJ/cm}^3$. Thus a theoretical energy efficiency mJ/mJ in this case is 10^{-2} . This scales as $(\text{THz}/f)^2$ with frequency. More importantly, the energy per Hz is larger by a factor of N (number of capacitors) than the broadband. Frequency tunability scaling is determined by (5). It is a linear function of energy. Using 10 mJ pulses, frequencies exceeding 10 THz can be generated. Finally, the bandwidth is controlled by the number of capacitors N so that $\Delta\omega/\omega = 1/N$. Besides using longer lengths, the bandwidth can be significantly decreased by implementing phased array concepts as shown in the above figures.

We have presented a proof-of-principle experiment of a novel radiation concept that can generate tunable, narrow-band radiation spanning the range of 100 GHz to the FIR. The concept is a hybrid, whose physics involves aspects of frozen wave generation, large aperture photoconducting antennas and frequency upshifting by superluminal plasma fronts. On the practical side we should remark that the use of photoconductors provides several advantages. The high breakdown threshold allows significant energy storage, and large radiated power consistent with the E_0^2 scaling of (6). The small energy bandgap reduces the required ionisation energy. Finally, the short recombination time allows a high repetition rate. The concept is fully scalable and has the potential for providing powerful, tunable sources in a frequency range valuable for many spectroscopic applications.

4 References

- GRISCHKOWSKY, D., KEIDING, S., VAN EXTER, M., and FATTINGER, Ch.: ‘Far-infrared time-domain spectroscopy with terahertz beams of dielectrics and semiconductors’, *J. Opt. Soc. Am. B, Opt. Phys.*, 1990, pp. 2006–2015
- GREENE, B.I., SAETA, P.N., DYKAAR, D.R., SCHMITT-RINK, S., and CHUANG, S.L.: ‘Far-infrared light generation at semiconductor

- surfaces and its spectroscopic applications', *IEEE J. Quantum Electron.*, 1992, **28**, pp. 2302-2312
- 3 ZHANG, X.C., and JIN, Y.: 'Perspectives in optoelectronics' (1995), Chap. 3, p. 81
 - 4 ZHANG, X.C., HU, B.B., DARROW, J.T., and AUSTON, D.J.: 'Generation of femtosecond electromagnetic pulses from semiconductor surfaces', *Appl. Phys. Lett.*, 1990, **56**, pp. 1011-1013
 - 5 ZHANG, X.C., DARROW, J.T., HU, B.B., AUSTON, D.H., SCHMIDT, M.T., THAM, P., and YANG, E.S.: 'Optically induced electromagnetic radiation from semiconductor surfaces', *Appl. Phys. Lett.*, 1990, **56**, pp. 2228-2230
 - 6 BENICEWICZ, P.K., ROBERTS, J.P., and TAYLOR, A.J.: 'Scaling of terahertz radiation from large-aperture biased photoconductors', *J. Opt. Soc. Am. B Opt. Phys.*, 1994, **11**, pp. 2533-2546
 - 7 AUSTON, D.H., CHEUNG, K.P., VALDMANIS, J.A., and KLEINMAN, D.A.: *Phys. Rev. Lett.*, 1984, **53**, pp. 1555
 - 8 FATTINGER, Ch., and GRISCHKOWSKY, D.: 'A Cherenkov source for freely-propagating terahertz beams', *IEEE J. Quantum Electron.*, 1989, **25**, pp. 2608-2610
 - 9 HU, B.B., ZHANG, X.C., AUSTON, D.H., and SMITH, P.R.: 'Free-space radiation from electro-optic crystals', *Appl. Phys. Lett.*, 1990, **56**, pp. 506-508
 - 10 CHUANG, S.L., SCHMITT-RINK, S., GREENE, B.I., SAETA, P.N., and LEVI, A.F.J.: 'Optical rectification at semiconductor surfaces', *Phys. Rev. Lett.*, 1992, **68**, pp. 102-105
 - 11 MILLER, D.A.B., CHEMLA, D.S., and SCHMITT-RINK, S.: *Phys. Rev. B*, 1986, **33**, p. 6976
 - 12 MORI, W.B., KATSOULEAS, T., DAWSON, J.M., and LAI, C.H.: 'Conversion of dc fields in a capacitor array to radiation by a relativistic ionization front', *Phys. Rev. Lett.*, 1995, **74**, pp. 542-545
 - 13 LAI, C.H., LIOU, R., and KATSOULEAS, T.C.: 'Demonstration of microwave generation from a static field by a relativistic ionization front in a capacitor array', *Phys. Rev. Lett.*, 1996, **77**, pp. 4764-4767
 - 14 VAN EXTER, M., FATTINGER, Ch., and GRISCHKOWSKY, D.: 'High-brightness terahertz beams characterized with an ultrafast detector', *Appl. Phys. Lett.*, 1989, **55**, pp. 337-339
 - 15 SEMENOVA, V.I.: *Sov. Radiophys. Quantum Electron.*, 1967, **10**, p. 599
 - 16 LAMPE, M., OTT, E., and WALKER, J.H.: *Phys. Fluids*, 1978, **10**, p. 42
 - 17 ESAREY, E., JOYCE, G., and SPANGLE, P.: 'Frequency up-shifting of laser pulses by copropagating ionization fronts', *Phys. Rev. A*, 1991, **44**, pp. 3908-3911
 - 18 GILDENBERG, V.B. *et al.*: *IEEE Trans. Plasma Sci.*, 1993, **21**, p. 34
 - 19 WILKS, S.C., DAWSON, J.M., and MORI, W.B.: *Phys. Rev. Lett.*, 1988, **61**, p. 337
 - 20 ESAREY, E., SPRANGLE, P., HAFIZY, B., and SERAFIM, P.: 'Radiation generation by photoswitched, periodically biased semiconductors', *Phys. Rev. E*, 1996, **53**, pp. 6419-6426